NASA/TM—2012-217697

Methods for Assessing Honeycomb Sandwich Panel Wrinkling Failures

Bart F. Zalewski and William B. Dial
ZIN Technologies, Middleburg Heights, Ohio

Brett A. Bednarcyk
Glenn Research Center, Cleveland, Ohio

October 2012

NASA STI Program . . . in Profile

Since its founding, NASA has been dedicated to the advancement of aeronautics and space science. The NASA Scientific and Technical Information (STI) program plays a key part in helping NASA maintain this important role.

The NASA STI Program operates under the auspices of the Agency Chief Information Officer. It collects, organizes, provides for archiving, and disseminates NASA's STI. The NASA STI program provides access to the NASA Aeronautics and Space Database and its public interface, the NASA Technical Reports Server, thus providing one of the largest collections of aeronautical and space science STI in the world. Results are published in both non-NASA channels and by NASA in the NASA STI Report Series, which includes the following report types:

- TECHNICAL PUBLICATION. Reports of completed research or a major significant phase of research that present the results of NASA programs and include extensive data or theoretical analysis. Includes compilations of significant scientific and technical data and information deemed to be of continuing reference value. NASA counterpart of peer-reviewed formal professional papers but has less stringent limitations on manuscript length and extent of graphic presentations.

- TECHNICAL MEMORANDUM. Scientific and technical findings that are preliminary or of specialized interest, e.g., quick release reports, working papers, and bibliographies that contain minimal annotation. Does not contain extensive analysis.

- CONTRACTOR REPORT. Scientific and technical findings by NASA-sponsored contractors and grantees.

- CONFERENCE PUBLICATION. Collected papers from scientific and technical conferences, symposia, seminars, or other meetings sponsored or cosponsored by NASA.

- SPECIAL PUBLICATION. Scientific, technical, or historical information from NASA programs, projects, and missions, often concerned with subjects having substantial public interest.

- TECHNICAL TRANSLATION. English-language translations of foreign scientific and technical material pertinent to NASA's mission.

Specialized services also include creating custom thesauri, building customized databases, organizing and publishing research results.

For more information about the NASA STI program, see the following:

- Access the NASA STI program home page at *http://www.sti.nasa.gov*

- E-mail your question to *help@sti.nasa.gov*

- Fax your question to the NASA STI Information Desk at 443–757–5803

- Phone the NASA STI Information Desk at 443–757–5802

- Write to:
  STI Information Desk
  NASA Center for AeroSpace Information
  7115 Standard Drive
  Hanover, MD 21076–1320

NASA/TM—2012-217697

Methods for Assessing Honeycomb Sandwich Panel Wrinkling Failures

Bart F. Zalewski and William B. Dial
ZIN Technologies, Middleburg Heights, Ohio

Brett A. Bednarcyk
Glenn Research Center, Cleveland, Ohio

National Aeronautics and
Space Administration

Glenn Research Center
Cleveland, Ohio 44135

October 2012

Level of Review: This material has been technically reviewed by technical management.

Available from

NASA Center for Aerospace Information
7115 Standard Drive
Hanover, MD 21076–1320

National Technical Information Service
5301 Shawnee Road
Alexandria, VA 22312

Available electronically at http://www.sti.nasa.gov

Methods for Assessing Honeycomb Sandwich Panel Wrinkling Failures

Bart F. Zalewski and William B. Dial
ZIN Technologies
Middleburg Heights, Ohio 44130

Brett A. Bednarcyk
National Aeronautics and Space Administration
Glenn Research Center
Cleveland, Ohio 44135

1.0 Introduction

This document presents the assessment of an accurate yet efficient method for predicting sandwich panel facesheet wrinkling using the wrinkling stress calculation developed by Heath (1960) and Vinson (1999) and the combined multiaxial failure criterion developed by Ley et al. (1999). These closed form predictions were verified using several finite element analyses with varying levels of detail described in this report. The closed form method was then implemented into the HyperSizer Structural Sizing Software (HyperSizer, 2012) as a user-defined failure criterion, and the implemented code was verified using hand calculations. The motivation for this work was the need for an accurate wrinkling solution that is also sufficiently computationally efficient so as to be implemented into sizing software, such as HyperSizer, for accurate and quick wrinkling assessment early in the structural design process.

Facesheet wrinkling, often referred to simply as wrinkling, is a failure mode that is commonly observed in sandwich panels with thin facesheets and lightweight cores, which do not provide a great deal of support to the facesheets. The failure is characterized by short wavelength buckling in one or both facesheets, as shown in Figure 1, and the failure is usually catastrophic soon after the onset of wrinkling (Collier Research Corporation, 2011). It is thus critical to account for this failure mode when designing sandwich panels for structural applications.

2.0 Closed Form Wrinkling Equations

The existing method in HyperSizer treats sandwich panel facesheet wrinkling as buckling of a simple beam on elastic foundation and predicts wrinkling failure based on a modification of the equation developed by Hemp (1948), which is the same equation developed by Yusuff (1955). The average wrinkling stress is given by,

$$sw = 0.82\, E_f \sqrt{\frac{E_c t_f}{E_f t_c}} \tag{1}$$

where E_f is the effective modulus of the facesheet, t_f is the facesheet thickness, E_c is the core through-thickness modulus, and t_c is the core thickness. The equation has shortcomings due to its beam assumption when it is used in an analysis of a plate, but it represents a good starting point approximation. The Heath equation is more appropriate for honeycomb panels and showed very good correlation with both simple and detailed finite element simulations (Vinson, 1999). The Heath (1960) equation was developed for an isotropic facesheet and is given by Vinson (1999) as,

$$sw = \sqrt{\frac{2 t_f E_c E_f}{3 t_c \left(1 - v_f{}^2\right)}} \tag{2}$$

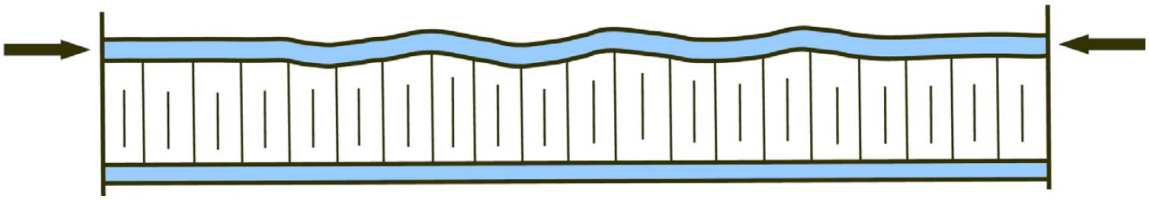

Figure 1.—Schematic illustration of the facesheet wrinkling failure mode in a sandwich panel (Collier Research Corporation, 2011).

where ν_f is the effective Poisson ratio of the facesheet. This equation can be modified for an anisotropic facesheet as (Vinson, 1999),

$$sw = \sqrt{\frac{2t_f E_c \sqrt{E_{fx} E_{fy}}}{3t_c\left(1 - \nu_{xy}\nu_{yx}\right)}} \tag{3}$$

where E_{fx} is the effective modulus of the facesheet in the 0° (x) direction, E_{fy} is the effective modulus of the facesheet in the 90° (y) direction, ν_{xy} is the xy Poisson ratio of the facesheet, and ν_{yx} is the yx Poisson ratio of the facesheet. Equation (3) is used in this report to predict the wrinkling stress.

Although Equation (3) is appropriate for the honeycomb construction and accounts for anisotropy of the facesheets, it does not consider a case where a plate is subjected to combined multiaxial loading. Real structures are almost always subjected to combined multiaxial loads, so they need to be accounted for in the wrinkling failure criterion. Ley et al. (1999) suggests two plane stress failure criteria developed by Sullins et al. (1969) and Bruhn (1973). The Sullins et al. (1969) wrinkling failure criterion can only be used if both of the principal stresses, in the plane of the facesheet, are compressive. The criterion is stated as (Ley et al., 1999),

$$\left(\frac{\sigma_1}{sw_1}\right)^3 + \frac{\sigma_2}{sw_2} = 1, \qquad \sigma_1 < \sigma_2 \le 0 \tag{4}$$

where σ_1 is the average major principal stress in the facesheet, σ_2 is the average minor principal stress in the facesheet, sw_1 is the corresponding average wrinkling stress allowable in the major principal direction, and sw_2 is the corresponding average wrinkling stress allowable in the minor principal direction. The Bruhn (1973) wrinkling failure criterion places no restrictions on the stress components, aside from requiring one normal stress component to be compressive. This criterion is stated as (Ley et al., 1999):

$$\frac{\sqrt[3]{\sigma_{xx}^3 + \sigma_{yy}^3}}{K\,sw} + \left(\frac{\tau_{xy}}{sw}\right)^2 = 1 \tag{5}$$

where σ_{xx} is the average 0° stress in the facesheet, σ_{yy} is the average 90° stress in the facesheet, τ_{xy} is the average shear stress in the facesheet, and K is a factor dependent on the direction of the largest applied compressive stress. If the largest compressive stress is parallel to the core ribbon direction $K = 1$, otherwise, $K = 0.95$. The Sullins et al. (1969) failure criterion was modified to account for Equation (3), which does not differentiate the wrinkling stress between principal directions as,

$$\left(\frac{\sigma_1}{sw}\right)^3 + \frac{\sigma_2}{sw} = 1, \qquad \sigma_1 < \sigma_2 \le 0 \tag{6}$$

The Bruhn (1973) equation was also modified with a conservative approach of always setting $K = 0.95$, resulting in,

$$\frac{\sqrt[3]{\sigma_{xx}^3 + \sigma_{yy}^3}}{0.95sw} + \left(\frac{\tau_{xy}}{sw}\right)^2 = 1 \tag{7}$$

3.0 Uniaxial Verification of Closed Form Wrinkling Equations

Equation (3) was verified first using simple plate finite element models that were subjected to uniaxial compression. For this verification study, an 8 in. wide by 11 in. high flat sandwich panel was considered. The results were checked for sensitivity to the through thickness mesh density of the core. The facesheets were constructed using a quasi-isotropic $[45/90/–45/0]_s$ layup of IM7/977-3 plies and a 1 in. thick core was considered as a 3.1 pcf 1/8-5052-.0007 aluminum honeycomb. The material properties of the facesheet plies are restricted and thus not provided herein. The core effective material properties are given in Table I.

TABLE I.—3.1 pcf 1/8-5052-.0007 ALUMINUM HONEYCOMB EFFECTIVE MATERIAL PROPERTIES

Property	Symbol	Value
Through-thickness tensile Young's modulus	Et	0.075 Msi
Through-thickness compressive Young's modulus	Ec	0.075 Msi
Transverse through-thickness shear modulus	Gw	0.022 Msi
Longitudinal through-thickness shear modulus	Gl	0.045 Msi
Through-thickness tensile strength	Ftu	0.215 ksi
Transverse through-thickness shear strength	Fsuw	0.09 ksi
Longitudinal through-thickness shear strength	Fsul	0.154 ksi
Stabilized through-thickness compressive strength	Fcus	0.215 ksi
Bare through-thickness compressive strength	Fcub	0.2 ksi
Through-thickness compressive crushed stress	Fcuc	0.13 ksi

The simple finite element models explicitly considered the through-thickness behavior, with the width of the panel (8 in.) being captured as the out-of-plane thickness of the elements. Since the facesheets in this analysis are quasi-isotropic, they were modeled using isotropic plates with equivalent, homogenized, elastic properties. All models (see Figure 3) consisted of facesheets with eight linear plane stress plate elements though the thickness, while the core was modeled using orthotropic plate elements to reflect the significant differences between axial and through-thickness properties. Both full and symmetric models were examined to observe the impact of the assumption of symmetry on the predicted wrinkling behavior. The boundary conditions are shown in Figure 2 and consisted of fixed constraints at the bottom edge, symmetry or free constraints on the sides, and applied vertical displacement at the top, with other displacement components constrained. Linear buckling and geometrically nonlinear static analyses were performed to ensure the validity of both of these types of solution. As will be shown, in general, they corresponded very well. The six finite element models used in this comparative study are described in Table II.

The applied global displacement at which wrinkling was predicted by the finite element models is given in Table II. For the linear buckling analyses, these values were calculated from the first eigenvalue returned by the finite element solver. For the nonlinear static analyses wrinkling displacement was taken as the displacement right before the load began to decrease. It should be noted that the onset of wrinkling was insensitive to the number of elements used through the thickness of the core, the assumption of symmetry, and linear buckling versus nonlinear analysis method. Figure 3 shows wrinkling shapes obtained from FEA. It should be noted that these are exaggerated to clarify the wrinkling mode shape.

Next, the closed form expression given by Equation (3) was used to perform a quick assessment of wrinkling for the honeycomb panel, and the result was compared with the wrinkling load predicted by

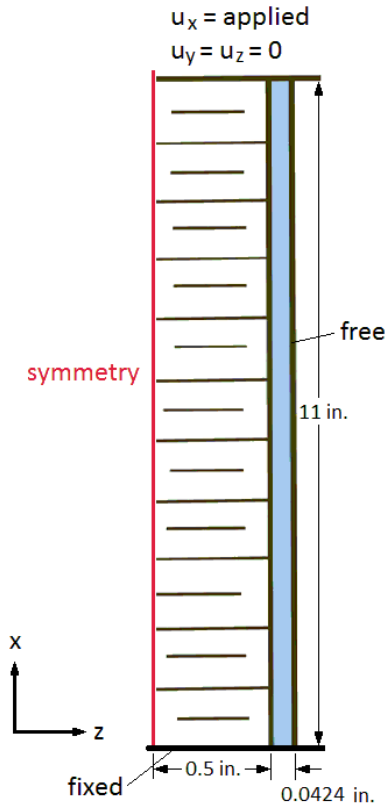

Figure 2.—Boundary conditions employed in the two-dimensional planar honeycomb sandwich finite element model.

TABLE II.—TWO-DIMENSIONAL PLANAR HONEYCOMB SANDWICH FINITE ELEMENT MODELS

Model number	Type	Elements through the facesheet thickness	Elements through the core	Analyses performed
1	Symmetric	8	20	Linear buckling Nonlinear static
2	Symmetric	8	8	Linear buckling
3	Symmetric	8	4	Linear buckling
4	Symmetric	8	2	Linear buckling
5	Full	8	1	Linear buckling Nonlinear static
6	Full	8	20	Linear buckling Nonlinear static

TABLE III.—COMPARISON OF THE TWO-DIMENSIONAL PLANAR HONEYCOMB SANDWICH FINITE ELEMENT MODELS AND THE MARGIN OF SAFETY (MOS) PREDICTED USING THE CLOSED FORM EXPRESSION

Model	Analysis type	Wrinkling displacement, in.	Closed form MOS
1	Linear buckling	0.1823088	0.0246
1	Nonlinear static	0.1925624	–0.0296
2	Linear buckling	0.1823032	0.0247
3	Linear buckling	0.1822670	0.0249
4	Linear buckling	0.1821046	0.0258
5	Linear buckling	0.1816686	0.0282
5	Nonlinear static	0.1900624	–0.0169
6	Linear buckling	0.1823088	0.0246
6	Nonlinear static	0.1930624	–0.0321

each finite element model. The margin of safety (MOS) associated with the closed form expression was calculated as the closed form equation wrinkling stress divided by the finite element model wrinkling stress minus 1. Thus, perfect agreement between the closed form expression and a given finite element model would yield a MOS of zero. The results, shown in Table III, illustrate a very good correlation between the observed wrinkling in finite element solutions and the closed form formulation of Equation (3) for the considered uniaxial loading. Compared to all six linear finite element analyses, the closed form expression provided a positive MOS, meaning the closed form expression was slightly non-conservative. Compared to the three nonlinear finite element analyses, the closed form expression was slightly conservative, with a negative MOS. The good agreement reported in Table III indicates potential for using this equation for wrinkling stress assessment in combined loading situations in conjunction with an appropriate multiaxial failure criterion.

Model	Wrinkling shapes
1 Linear	
1 Nonlinear	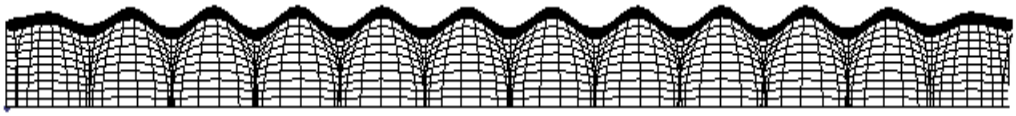
2 Linear	
3 Linear	
4 Linear	
5 Linear	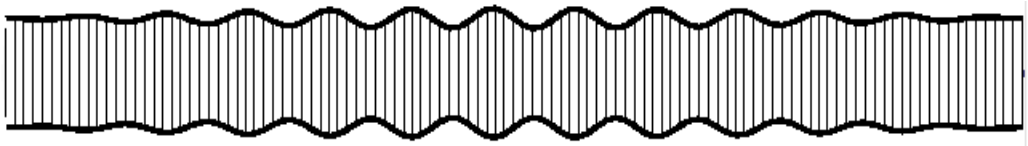
5 Nonlinear	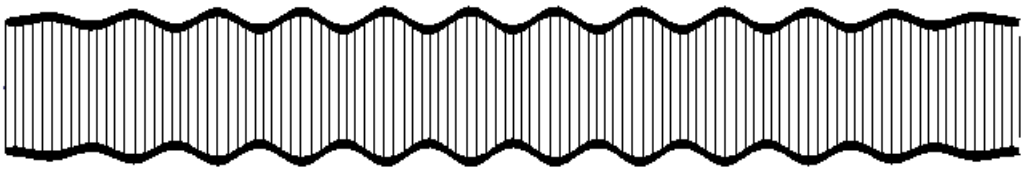
6 Linear	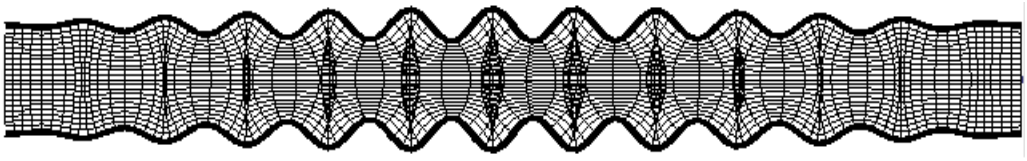
6 Nonlinear	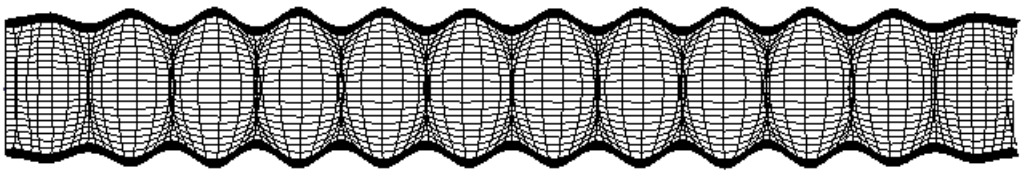

Figure 3.—Wrinkling shapes for each two-dimensional planar finite element analysis.

4.0 Multiaxial Verification of Closed Form Wrinkling Equations

To assess wrinkling in a panel where combined loading is present, two detailed finite element models were constructed that explicitly model the cell-level details of the core aluminum honeycomb. Both models were symmetric in the 8 in. width direction of the panel (i.e., 4 in. width analyzed), see Figure 4. The boundary conditions consisted of a fixed bottom edge, symmetry constraint on one of the sides, and an applied vertical displacement at the top, with the other displacement components constrained. Although only a uniaxial displacement was applied, the corners of the panel experienced multiaxial state of stress as the panel's Poisson effect expansion (y-direction) is constrained by the fixed boundary conditions at the top and the bottom. The facesheets were modeled using plate elements with explicit $[45/90/-45/0]_s$ layups, and the core was modeled using isotropic plate elements with Al 5052 properties (E = 10.2 Msi, ν = 0.33). Four elements were used through the core thickness. The first model included nonlinear spring elements between core and facesheets to model the contribution of adhesive and account for the different core stiffness in tension and compression. The compressive spring stiffness was restricted from displacing more than half the facesheet thickness. The model was subjected to a nonlinear static analysis that consisted of 10 steps with the structural stiffness matrix being updated at each iteration. Additional details of the finite element model are shown in Figure 5.

In the first model, the stiffness of the springs used to model the adhesive was calibrated using a 2- by 2-in. model, constructed similarly to the above model, such that the tensile and compressive stiffness matched through thickness tension and compression test results (Lerch, 2011). In these tests, the average core through thickness tensile and compressive Young's moduli were 44 and 80 ksi, respectively. The calibration procedure resulted in the following tensile (k_t), compressive (k_c), and shear (k_s) spring stiffnesses,

$$k_t = k_s = 774.8 \text{ lb/in.}$$

$$k_c = \begin{cases} 1379 \text{ lb/in.}, & u_z \geq -0.0212 \\ 1.022 \times 10^6 \text{ lb/in.}, & u_z < -0.0212 \end{cases} \tag{8}$$

The nonlinear progressive collapse analysis resulted in the through thickness displacements shown in Figure 6. The figure shows out-of-plane displacement contours and total displacement shapes at various global displacements, which are noted on the figure.

The model results show progressive collapse, which mimics a wrinkling type failure, as would be expected. The strains at the top and bottom corners of the panel were monitored to determine the displacement at which the panel wrinkled. Since wrinkling is a facesheet buckling phenomena, strains on the outside and on the core side of a single facesheet were considered. For global buckling one would need to consider strains on both facesheets. The strain data are plotted in Figure 7 for the corner point indicated with a circle in Figure 6.The point at which the panel wrinkled was determined as the point at which the principal strain reverses slope and remains reversed (Singer et al., 1998) (Figure 7).

The first detailed model took approximately 64 hr to run on a 32 bit Windows PC using the NASTRAN finite element code.

The second detailed model took into account differences between the through thickness tensile and compressive properties of the core by modeling the elastic modulus of the core aluminum material as a nonlinear property calibrated to match the aforementioned experimental results. This was meant to alleviate a slight penetration of the facesheet into the core observed in the first detailed model. A tensile modulus of 3.438 Msi and a compressive modulus of 6.250 Msi resulted from the calibration procedure. The second detailed model was subjected to a nonlinear static analysis that consisted of 10 steps with the stiffness matrix being updated at each iteration. The model was the same as before except for the facesheet having coincidental nodes with the core, instead of facesheet and core being connected through nonlinear spring elements.

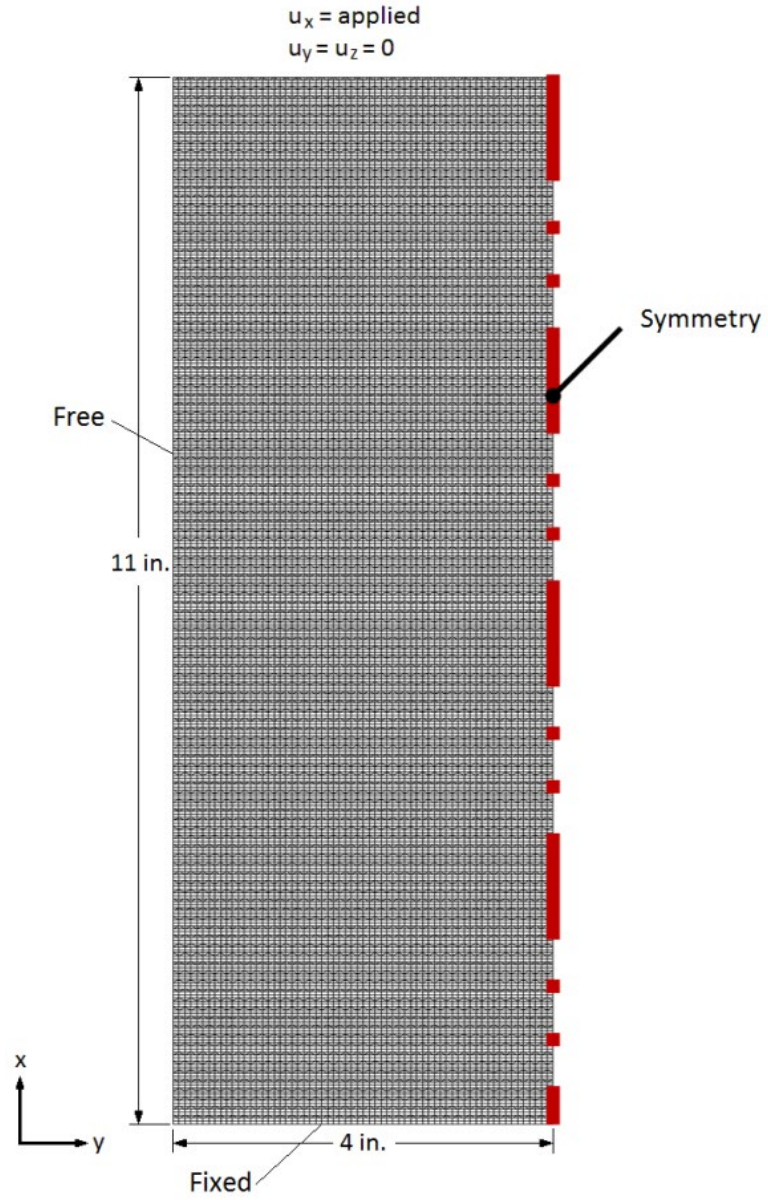

Figure 4.—Detailed finite element model of the honeycomb sandwich panel.

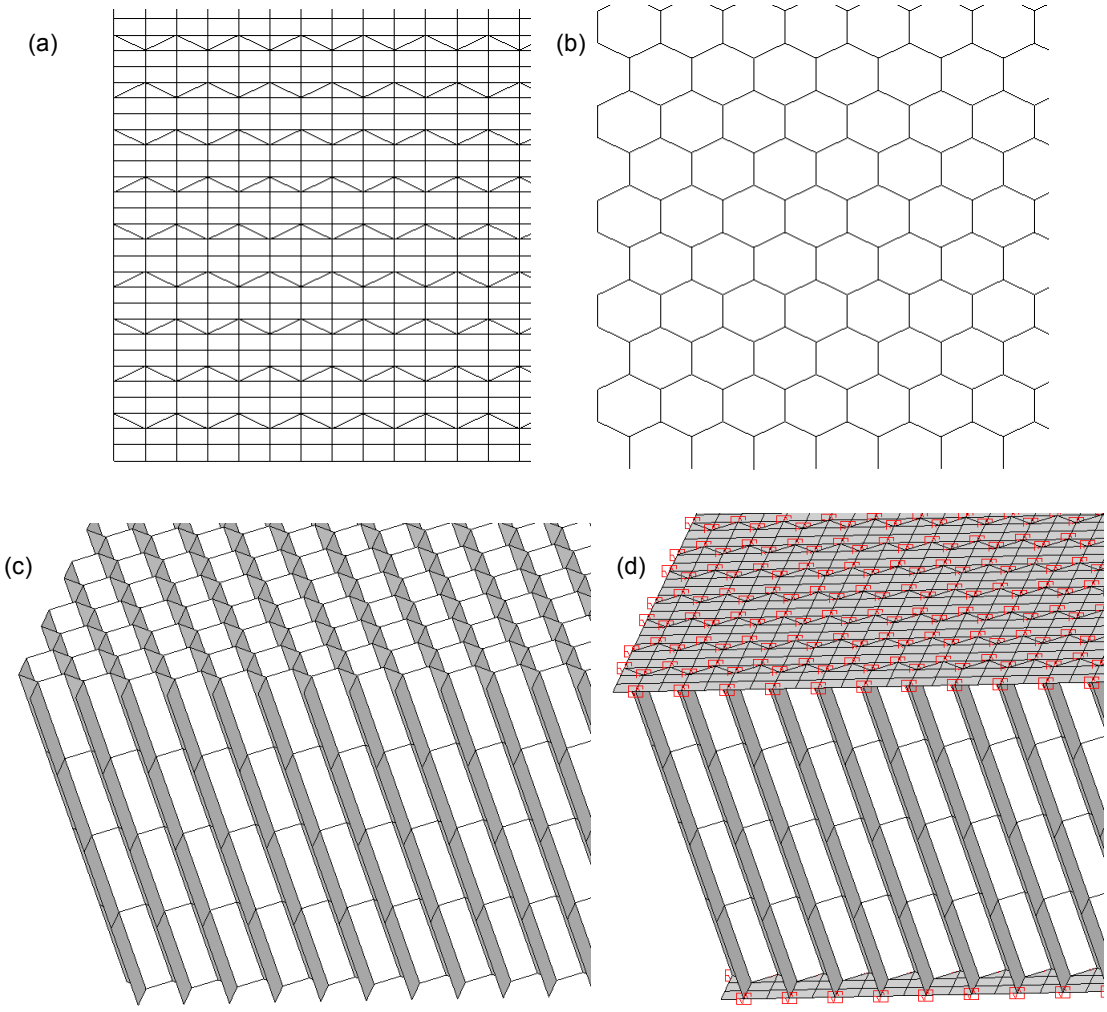

Figure 5.—Details of the finite element model mesh. (a) Through thickness view with facesheet. (b) Through thickness view without facesheet. (c) Isoparametric view with facesheet. (d) Isoparametric view with facesheet.

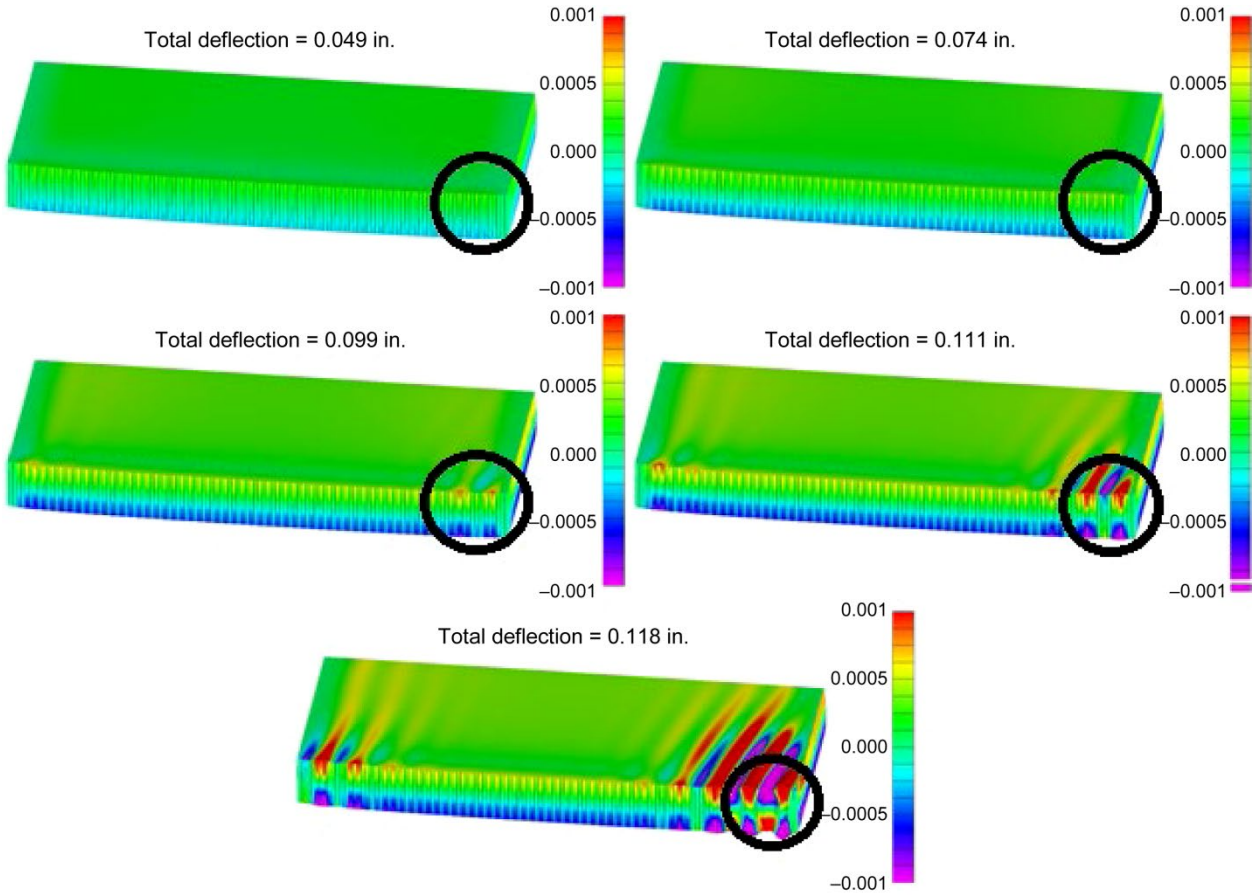

Figure 6.—Progressive wrinkling deformation of the detailed model utilizing nonlinear springs to model the adhesive between the facesheet and core.

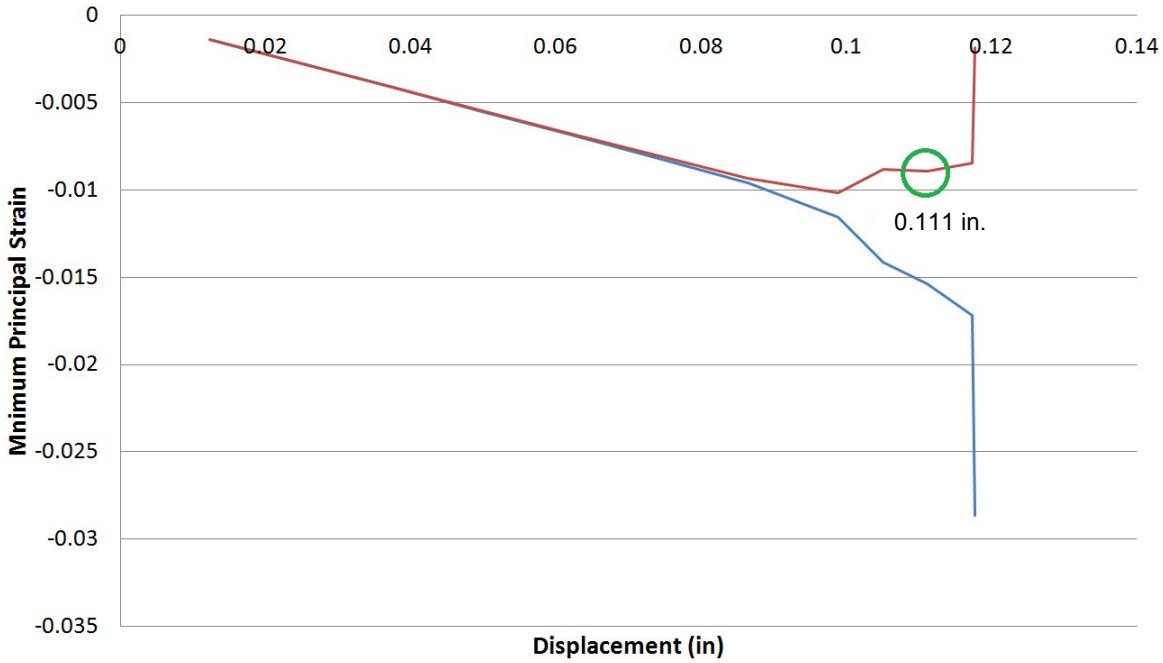

Figure 7.—Determination of wrinkling point in the first detailed finite element model.

The nonlinear progressive analysis resulted in the through thickness displacements shown in Figure 8. The figure shows out-of-plane displacement contours and total displacement shapes at various global displacements, which are indicated on the figure. Note that these global displacement levels are not the same as those shown in Figure 6, although both Figure 6 and Figure 8 include a figure at the displacement associated with the simulated buckling point.

As in the first model, the second model results show progressive collapse, which mimics a wrinkling type failure, as would be expected. As before, the strains at the top and bottom of the panel were monitored to determine the displacement at which the panel wrinkled, see Figure 9. The point plotted in Figure 9 is indicated with the circle in Figure 8.

The second detailed model took approximately 68.5 hr to run on a 32 Windows PC using the NASTRAN finite element software.

Since wrinkling is a local buckling phenomena, the method for wrinkling failure determination was used similar to that used for global buckling. The point at which the strain slope reversed was considered as failure (Singer et al., 1998) (Figure 9).

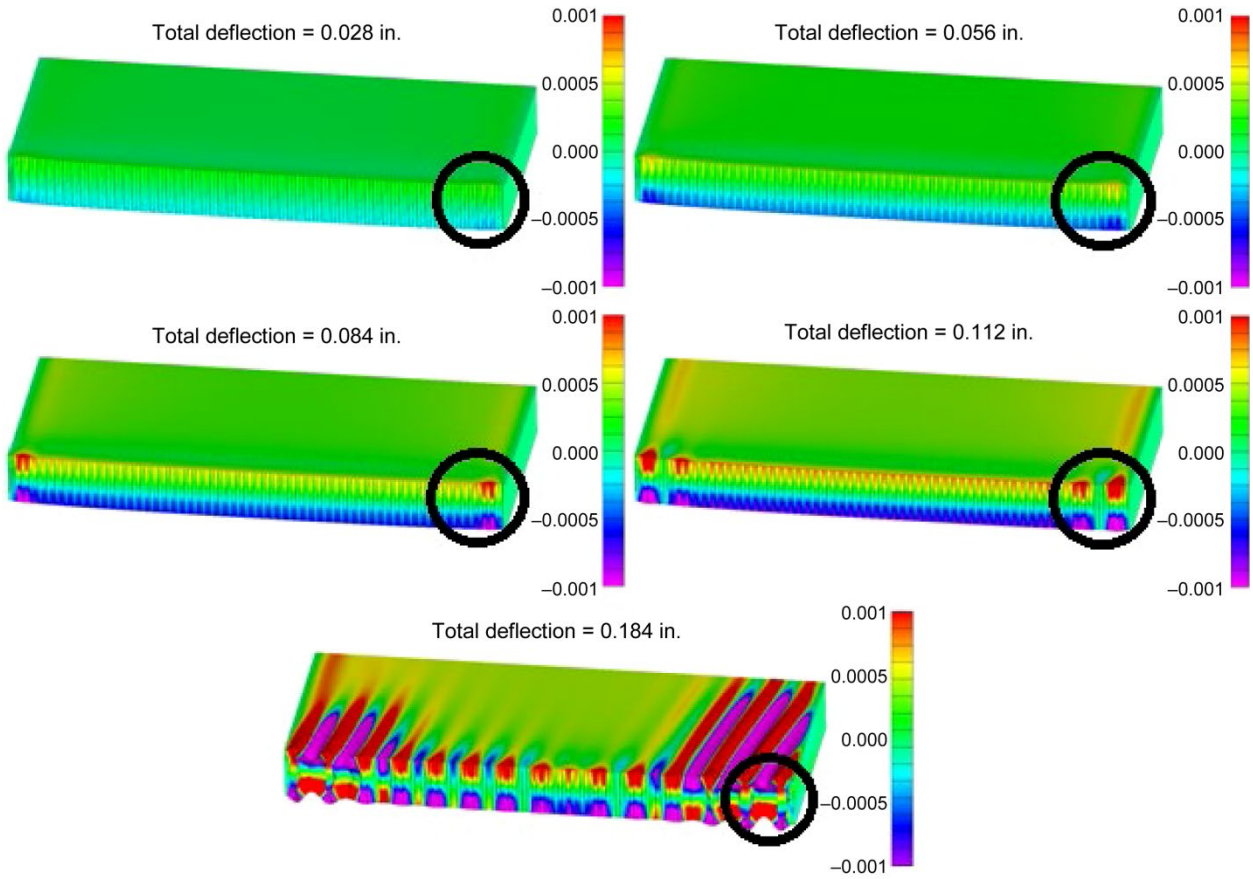

Figure 8.—Progressive wrinkling deformation of the detailed model utilizing coincident nodes between the facesheet and core and distinct tensile and compressive moduli for the core aluminum material.

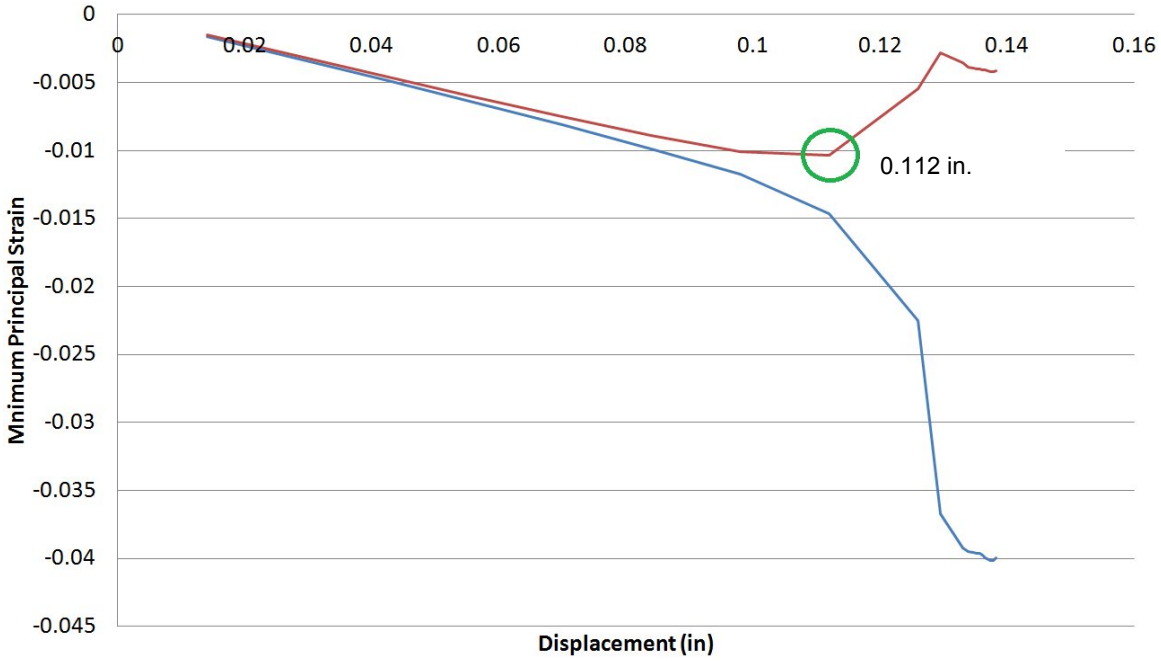

Figure 9.—Determination of wrinkling point in the second detailed finite element model.

5.0 HyperSizer Implementation

The two detailed models were compared to a laminated plate model with a layup consisting of the entire sandwich stack up, see Figure 10. A model like this can be used in HyperSizer to perform sizing analysis iterations and failure analyses. The model a fixed bottom edge with the applied vertical displacement at the top edge, while other displacement components at the top edge were constrained. Two displacements were applied, each corresponding to a wrinkling displacement from the detailed models, namely 0.111 and 0.112 in. The element forces were imported into HyperSizer to perform the built in wrinkling analysis.

The wrinkling margins predicted by HyperSizer using the existing Hemp (1948) Equation (1) for the applied displacements of 0.111 and 0.112 in. are displayed in Figure 11 and Figure 12.

The existing HyperSizer method based on the Hemp (1948) equation provides a highly negative margin of safety, indicating the high degree of conservatism compared to the detailed finite element model results. Equations (3), (6), and (7) were implemented into HyperSizer as a user defined failure criterion. This requires the user to provide a dynamically linked library (.dll) of the code that returns a margin of safety to HyperSizer. Thus, two margin of safety equations were developed based on formulation provided by Chambers (1995). The margins of safety (MOS) associated with Equations (6) and (7) can be written as,

$$\mathrm{MOS} = \frac{1}{\sqrt{\left(\frac{\sigma_1}{sw}\right)^3 + \frac{\sigma_2}{sw}}} - 1, \qquad \sigma_1 < \sigma_2 \le 0 \tag{9}$$

$$\mathrm{MOS} = \frac{1}{\sqrt{\frac{\sqrt[3]{\sigma_{xx}^3 + \sigma_{yy}^3}}{0.95sw} + \left(\frac{\tau_{xy}}{sw}\right)^2}} - 1 \tag{10}$$

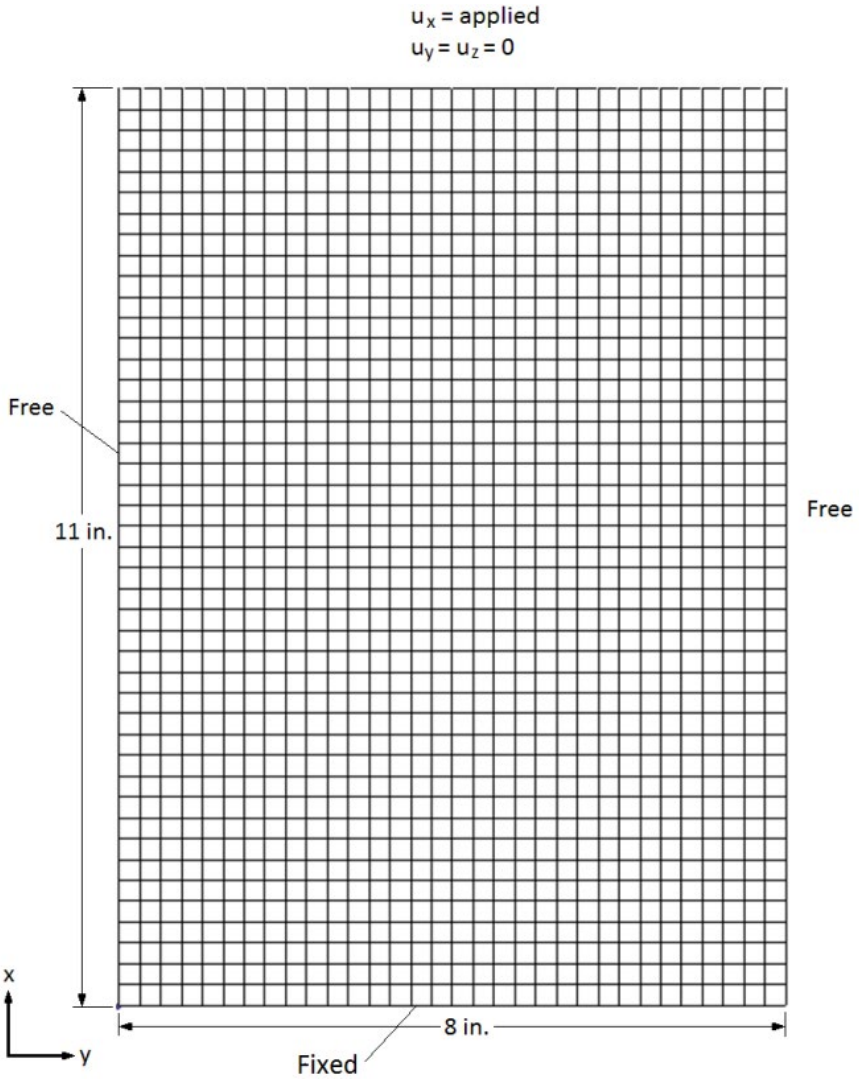

Figure 10.—Laminate plate finite element model used for HyperSizer evaluation.

Ultimate MS	γ	LS	Location – Analysis Description
–0.3376 (0)		1	**Top Honeycomb Face** Wrinkling, Eq. (2), Honeycomb or RCS Core, X, Y, and Interaction
–0.3376 (0)		1	**Bottom Honeycomb Face** Wrinkling, Eq. (2), Honeycomb or RCS Core, X, Y, and Interaction

Figure 11.—Wrinkling margins of safety for the first detailed model using the existing HyperSizer method.

Ultimate MS	γ	LS	Location – Analysis Description
–0.3426 (0)		1	**Top Honeycomb Face** Wrinkling, Eq. (2), Honeycomb or RCS Core, X, Y, and Interaction
–0.3426 (0)		1	**Bottom Honeycomb Face** Wrinkling, Eq. (2), Honeycomb or RCS Core, X, Y, and Interaction

Figure 12.—Wrinkling margins of safety for the second detailed model using the existing HyperSizer method.

Ultimate MS	γ	LS	Location – Analysis Description
0.0652 (0)		1	**Top Honeycomb Face** Sandwich Face, User Defined #1
0.0652 (0)		1	**Bottom Honeycomb Face** Sandwich Face, User Defined #1

Figure 13.—Wrinkling margins of safety for the first detailed model using the newly implemented HyperSizer method.

Ultimate MS	γ	LS	Location – Analysis Description
0.05423 (0)		1	**Top Honeycomb Face** Sandwich Face, User Defined #1
0.05423 (0)		1	**Bottom Honeycomb Face** Sandwich Face, User Defined #1

Figure 14.—Wrinkling margins of safety for the second detailed model using the newly implemented HyperSizer method.

The margins of safety calculated using this new method for the wrinkling displacements determined from the two detailed finite element models are given in Figure 13 and Figure 14. It is evident that the new failure margins of safety correspond very well with the detailed finite element analyses, although they are slightly non-conservative. This non-conservatism could be handled with a knock-down or correction factor when using this method in design. It is also noteworthy that the discrepancy between the new closed form method and the detailed finite element results for this case that includes multiaxial loads are approximately twice those observed in the pure uniaxial cases reported in Table III. The run time for the entire analysis was on the order of few minutes due to the computational efficiency of the HyperSizer process.

6.0 Conclusion

This report has presented the verification of a set of closed form equations that can be used to predict the facesheet wrinkling failure of sandwich panels. Based on the work of Sullins et al. (1969), Bruhn (1973), and Ley et al. (1999), these equations admit anisotropic facesheet properties and multiaxial loading. The equations were implemented within the HyperSizer Structural Sizing Software (HyperSizer, 2012) such that they can be used in sizing structures to evaluate wrinkling failures in sandwich panel structural applications. The equations were compared to linear and nonlinear simplified plane finite element models for wrinkling of a realistic IM7/977-3 facesheet, aluminum honeycomb core sandwich panel for uniaxial loading, as well detailed finite element models of the panel that explicitly model the honeycomb structure for multiaxial loading. The new wrinkling assessment equations matched very well with the finite element results for uniaxial loading. For multiaxial loading, the equations were shown to be still in very good agreement with the detailed finite element results (although slightly non-conservative), and in much better agreement than the existing wrinkling assessment methodology within HyperSizer.

References

Bruhn E. F., “Analysis and Design of Flight Vehicle Structures,” Tri-State Offset Company, pp. C12.1-C12.52, 1973.

Chambers, J. A., “Preloaded Joint Analysis Methodology for Space Flight Structures,” NASA TM–106943, 1995.

Collier Research Corporation, “Methods and Equations for Sandwich Panel Facesheet Wrinkling,” HyperSizer Structural Sizing Software Documentation, 2011.

Heath, W. G., “Sandwich Construction, Part 2: The Optimum Design of Flat Sandwich Panels,” Aircraft Engineering, 1960.

Hemp, W. S., "On a Theory of Sandwich Construction," ARC Technical Report R&M 2672, 1948.
HyperSizer Structural Sizing Software, Collier Research Corp., Newport News, VA, www.HyperSizer.com, 2012.
Lerch B. A., Personal Communication, NASA Glenn Research Center, 2011.
Ley, R. P., Lin, W., and Mbanefo, U.., "Facesheet Wrinkling in Sandwich Structures," NASA/CR—1999-208994, 1999.
Singer J., Arbocz, J., T. Weller, T. "Buckling Experiments: Experimental Methods in Buckling of Thin-Walled Structures," Wiley, 1998.
Sullins, R. T., Smith G. W., and Spier, E. E., "Manual for Structural Stability Analysis of Sandwich Plates and Shells," NASA CR–1457, 1969.
Vinson, J. R., The Behavior of Sandwich Structures of Isotropic and Composite Materials, Technomic Publishing Co., Lancaster, PA, 1999.
Yusuff, S., "Theory of Wrinkling in Sandwich Construction," Journal of the Royal Aeronautical Society, Vol. 59, pp. 30-36, 1955.

REPORT DOCUMENTATION PAGE

Form Approved
OMB No. 0704-0188

1. REPORT DATE *(DD-MM-YYYY)*
01-10-2012

2. REPORT TYPE
Technical Memorandum

3. DATES COVERED *(From - To)*

4. TITLE AND SUBTITLE
Methods for Assessing Honeycomb Sandwich Panel Wrinkling Failures

5a. CONTRACT NUMBER

5b. GRANT NUMBER

5c. PROGRAM ELEMENT NUMBER

6. AUTHOR(S)
Zalewski, Bart, F.; Dial, William, B.; Bednarcyk, Brett, A.

5d. PROJECT NUMBER

5e. TASK NUMBER

5f. WORK UNIT NUMBER
WBS 944244.04.02.03

7. PERFORMING ORGANIZATION NAME(S) AND ADDRESS(ES)
National Aeronautics and Space Administration
John H. Glenn Research Center at Lewis Field
Cleveland, Ohio 44135-3191

8. PERFORMING ORGANIZATION REPORT NUMBER
E-18384

9. SPONSORING/MONITORING AGENCY NAME(S) AND ADDRESS(ES)
National Aeronautics and Space Administration
Washington, DC 20546-0001

10. SPONSORING/MONITOR'S ACRONYM(S)
NASA

11. SPONSORING/MONITORING REPORT NUMBER
NASA/TM-2012-217697

12. DISTRIBUTION/AVAILABILITY STATEMENT
Unclassified-Unlimited
Subject Category: 39
Available electronically at http://www.sti.nasa.gov
This publication is available from the NASA Center for AeroSpace Information, 443-757-5802

13. SUPPLEMENTARY NOTES

14. ABSTRACT
Efficient closed-form methods for predicting the facesheet wrinkling failure mode in sandwich panels are assessed. Comparisons were made with finite element model predictions for facesheet wrinkling, and a validated closed-form method was implemented in the HyperSizer structure sizing software.

15. SUBJECT TERMS
Wrinkling; Finite element method; Buckling; Nonlinearity; Failure; Honeycomb structures; Sandwich structures; Mathematical models; Structural design; Failure modes; Anisotropy; Compression loads; NASTRAN; Laminates; Simulation

16. SECURITY CLASSIFICATION OF:			17. LIMITATION OF ABSTRACT	18. NUMBER OF PAGES	19a. NAME OF RESPONSIBLE PERSON
a. REPORT	b. ABSTRACT	c. THIS PAGE			STI Help Desk (email:help@sti.nasa.gov)
U	U	U	UU	22	19b. TELEPHONE NUMBER *(include area code)* 443-757-5802

Standard Form 298 (Rev. 8-98)
Prescribed by ANSI Std. Z39-18